Christoph Reißer (Autor)

Finite Lifetime Effects in Top Quark Pair Production at Threshold

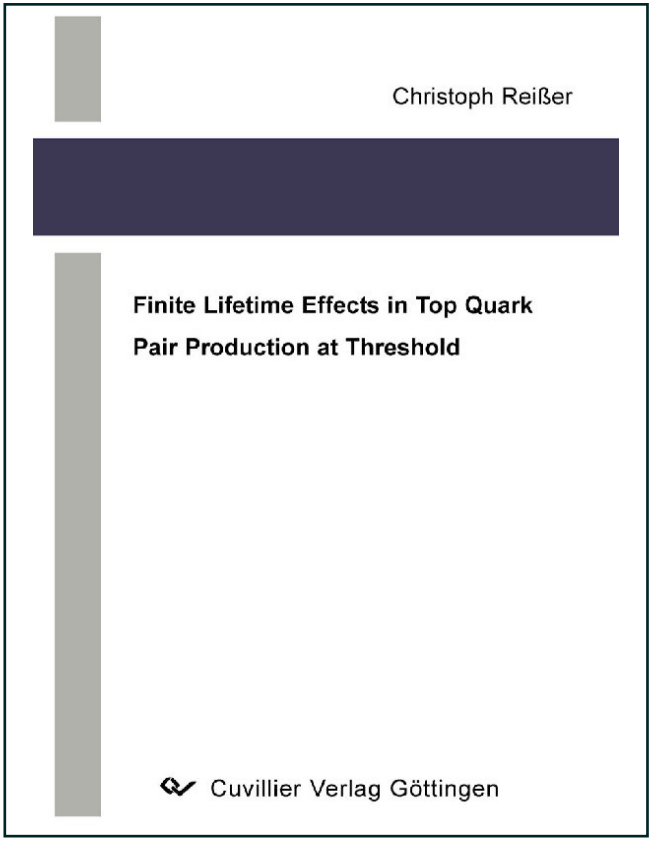

https://cuvillier.de/de/shop/publications/1451

Chapter 1

Non-Relativistic Top-Antitop Dynamics and the Effective Theory

1.1 Theoretical Motivation

The collision of electrons and positrons with a c. m. energy around two times the top quark mass, $\sqrt{s} \approx 344 \pm 5$ GeV, allows for a threshold production of top-antitop ($t\bar{t}$) pairs, i. e. heavy quarks of non-relativistic velocity

$$v = \sqrt{1 - \frac{4m_t^2}{s}} \ll 1$$

in the c. m. frame. In Fig. 1.1 the tree-level electroweak Standard Model process of e^+e^- annihilation and $t\bar{t}$ production via virtual photon or Z boson exchange is shown. In the non-relativistic energy regime, usual quantum chromodynamics (QCD) perturbation theory, in which the strong coupling α_s is the only expansion parameter, breaks down due to Coulomb singularities related to the binding of quark-antiquark pairs via the strong interaction: These arise as $(\alpha_s/v)^n$ terms in the loop expansion of the $t\bar{t}$ production current indicating that the instantaneous

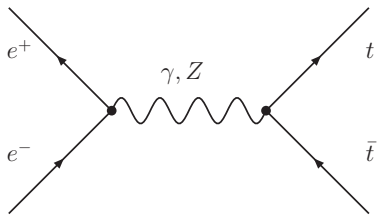

Figure 1.1: Standard Model tree-level $e^+e^- \to t\bar{t}$ diagrams.

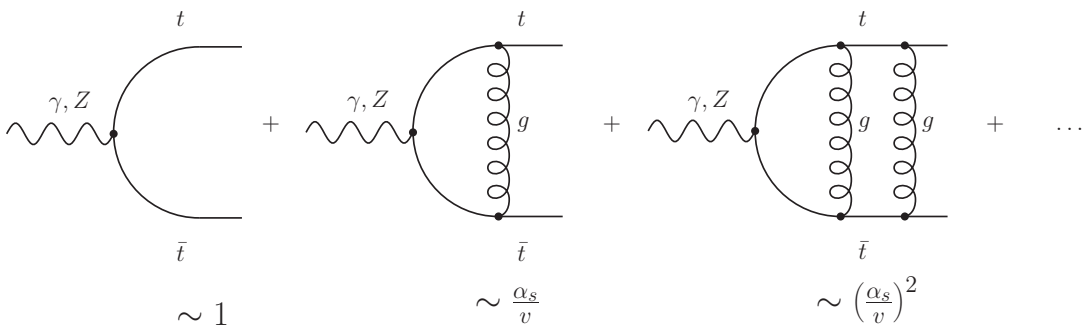

Figure 1.2: Loop expansion of the $t\bar{t}$ production current.

exchange of n time-like gluons between top and antitop, which come with a suppression of α_s^n, is associated with an enhancement factor of $(1/v)^n$, see Fig. 1.2. As a consequence it is not sufficient to cut the perturbation series at a finite order in α_s. Besides the large $(\alpha_s/v)^n$ terms, at the same time there are large logarithms of the velocity $(\alpha_s \ln v)^m$, which have to be accounted for in the theoretical description. By means of renormalization group methods it is possible to sum up such logarithms.

Another important feature of the non-relativistic top quark pair dynamics is the decay of the top and the antitop via the electroweak interaction. Because the Cabibbo-Kobayashi-Maskawa (CKM) matrix element V_{tb} is approximately one in the Standard Model, the top quark decays predominantly into a bottom quark and a W boson, $t \to bW$. The total decay width of the top, $\Gamma_t \approx 1.5$ GeV, is extraordinarily large compared to the other quarks and, in particular, larger than the hadronization scale, $\Gamma_t > \Lambda_{\mathrm{QCD}}$. Therefore top and antitop quarks decay even before hadronization takes place, so that toponium bound states cannot be formed. As a consequence, the $e^+e^- \to t\bar{t}$ threshold cross section as a function of the c. m. energy does not exhibit many individual bound state resonances, but rises smoothly when $t\bar{t}$ production becomes kinematically allowed. Another welcome implication of the decay being faster than hadronization is that non-perturbative effects can be assumed to be suppressed [4, 36].

The solution to the above mentioned problems of Coulomb singularities and large logarithms is to go from usual QCD perturbation theory to an effective theory which respects and carries the characteristics of the non-relativistic energy regime and hence contains the relevant degrees of freedom and the proper power counting. Apart from that also the fast top quark decay is taken into account by the effective theory. Such a theory is generically called non-relativistic QCD (NRQCD). In this work we use a particular version of NRQCD called velocity NRQCD (vNRQCD) [24, 25].

1.2 Energy Scales, Power Counting, Degrees of Freedom

Non-relativistic $t\bar{t}$ dynamics is governed by different energy scales, namely the hard scale of the top mass $m_t \approx 172$ GeV, the soft scale of the top 3-momentum $\mathbf{p} \sim m_t v \approx 25$ GeV and the ultrasoft scale of the kinetic energy $E \sim mv^2 \approx 3-4$ GeV of the $t\bar{t}$ system, where $E = \sqrt{s} - 2m_t$. The decay width is at the same order of magnitude as the kinetic energy and therefore also of the ultrasoft scale. Finally, the QCD hadronization scale $\Lambda_{\rm QCD}$ is below the ultrasoft scale. Due to the small velocity we have the separation

$$m_t \;\gg\; m_t v \;\gg\; \Gamma_t \sim m_t v^2 \;>\; \Lambda_{\rm QCD}\,. \tag{1.1}$$

This ordering holds even at threshold where the quarks are at rest. This is a consequence of the replacement $E \to E + i\Gamma_t$ [36] leading to $m_t v^2 = E + i\Gamma_t$ and therefore the absolute value of the effective velocity is bounded below. Thus, Γ_t serves as an infrared cutoff which prohibits non-perturbative dynamics that take place at $\Lambda_{\rm QCD}$.

From the comparison of these energy scales, one immediately obtains a power counting, which allows for a classification of the different contributions (e. g. loop diagrams) to a quantity (e. g. operator coefficients or the cross section) according to their expected numerical importance. In analogy to the Hydrogen atom one can assume a balance of kinetic energy $E \sim m_t v^2$ and potential energy $\sim m_t \alpha_s^2$ in the $t\bar{t}$ system. This leads to a relation between the velocity and the strong coupling. The counting of electroweak effects results from the numerical relation $\Gamma_t \sim m_t \alpha \approx E \sim m_t v^2$, where α is the fine structure constant. Altogether we obtain

$$E/m_t \sim v^2\,, \qquad \alpha_s \sim v\,, \qquad \Gamma_t/m_t \sim \alpha \sim v^2 \tag{1.2}$$

and use v as the counting parameter. As an example we consider the QCD contributions to the threshold cross section. They can be written in the schematic form

$$\begin{aligned} R = \frac{\sigma_{\rm thr}}{\sigma_{\mu^+\mu^-}} &= v \sum_{n,m} \left(\frac{\alpha_s}{v}\right)^n (\alpha_s \ln v)^m \\ &\quad \times \{1\,(\text{LL});\, v, \alpha_s\,(\text{NLL});\, v^2, \alpha_s v, \alpha_s^2\,(\text{NNLL})\}\,, \end{aligned}$$

where $(\alpha_s/v)^n$ and $(\alpha_s \ln v)^m$ terms are summed. We do not show terms beyond NNLL order here. Electroweak effects including phase space effects are also not written down at this point and will be discussed later.

The important momentum regions that follow from the physical energy scales

are [46]

$$\begin{aligned}
&\text{hard:} && (p^0, \mathbf{p}) \sim (m_t, m_t)\,, \\
&\text{soft:} && (p^0, \mathbf{p}) \sim (m_t v, m_t v)\,, \\
&\text{potential:} && (p^0, \mathbf{p}) \sim (m_t v^2, m_t v)\,, \\
&\text{ultrasoft:} && (p^0, \mathbf{p}) \sim (m_t v^2, m_t v^2)
\end{aligned}$$

with the notation $(p^0, \mathbf{p})$ = (energy, 3-momentum). The effective theory contains only those quark and gluonic degrees of freedom that can become on-shell for scales below the hard scale. These on-shell degrees of freedom are gluons and massless quarks in the soft and ultrasoft momentum region, and top quarks in the potential momentum region, referred to also as heavy quarks. Although soft gluons cannot be produced in the non-relativistic $t\bar{t}$ system of a kinetic energy $E \sim m_t v^2$, they are needed as relevant degrees of freedom since they are involved in the renormalization of effective theory operators. All off-shell fluctuations such as hard quarks and gluons, potential gluons and soft quarks in the QCD case are accounted for by on-shell matching of vNRQCD to full QCD at the hard scale. Electroweak effects are treated in the same way by on-shell matching to the full electroweak theory, as we will see in the following chapters. This matching fixes the Wilson coefficients of the effective theory operators at the hard scale.

The vNRQCD soft and ultrasoft fluctuations are separated from each other by means of a multipole expansion [47, 48] in analogy to heavy quark effective theory [49]. Ultrasoft momenta are continuous variables, whereas soft momenta appear as discrete labels for potential quarks and soft gluons, so that there exists an individual operator for each soft momentum. SU(3) gauge invariance, which is still present for ultrasoft energies and momenta, must be recovered for the soft energies and momenta through reparametrization invariance [24].

The regularization of loop integrals appearing in vNRQCD matrix elements is achieved by dimensional regularization [50–52] in $d = 4 - 2\epsilon$ dimensions. Renormalization is done in the modified minimal subtraction scheme $\overline{\text{MS}}$ [53–57]. The subtlety in applying dimensional regularization to vNRQCD diagrams is that for the ultrasoft integrals an ultrasoft regularization parameter μ_U has to be used, whereas for the soft and potential integrals one has to use a soft parameter μ_S [24]. These parameters are not independent, because the soft and the ultrasoft scales are related, and thus $\mu_S^2 = m_t \mu_U$. Therefore one can define $\mu_S = m_t \nu$ and $\mu_U = m_t \nu^2$, where ν is called the subtraction point velocity. By means of a renormalization group equation for ν it is possible to scale the Wilson coefficients of the effective theory from the hard matching scale $\mu_S = \mu_U = m_t$ down to $\mu_S = m_t v$, $\mu_U = m_t v^2$, i. e. from $\nu = 1$ to $\nu = v$. In the calculation of matrix elements involving gluon loops one encounters logarithms of the form

$$\ln \frac{\mu_U}{E} = \ln \frac{m_t \nu^2}{m_t v^2}, \quad \ln \frac{\mu_S}{\sqrt{m_t E}} = \ln \frac{m_t \nu}{m_t v}\,,$$

which are large at the hard scale $\nu = 1$. By choosing instead the scale $\nu \sim v$ these logarithms of the ultrasoft and the soft energy are rendered small simultaneously, their contribution shifted from the matrix elements to the Wilson coefficients. In this way the use of an effective theory has solved the above mentioned problem of large logarithms.

1.3 Effective QCD Lagrangian

The vNRQCD Lagrangian contains ultrasoft, soft and potential QCD components, $\mathcal{L}_{\rm QCD} = \mathcal{L}_u + \mathcal{L}_s + \mathcal{L}_p$, given in Refs. [24–27, 48]. The ultrasoft piece reads

$$\mathcal{L}_u = \sum_{\mathbf{p}} \psi^\dagger_{\mathbf{p}} \Big\{ iD^0 - \frac{(\mathbf{p} - i\mathbf{D})^2}{2m_t} + \frac{\mathbf{p}^4}{8m_t^3} + \frac{i}{2}\Gamma_t \left(1 - \frac{\mathbf{p}^2}{2m_t^2}\right) - \delta m_t + \dots \Big\} \psi_{\mathbf{p}} + (\psi_{\mathbf{p}} \to \chi_{\mathbf{p}}) - \frac{1}{4} G_u^{\mu\nu} G^u_{\mu\nu} + \dots \,, \tag{1.3}$$

where $G_u^{\mu\nu}$ is the ultrasoft field strength tensor and $\psi_{\mathbf{p}}$, $\chi_{\mathbf{p}}$ are heavy quark and antiquark two-component spinor fields of the soft momentum $\mathbf{p}$, respectively. The covariant derivative has the form $D^\mu = \partial^\mu + ig_u A^\mu$ with the renormalized ultrasoft QCD coupling $g_u = g_u(\mu_U)$ and the ultrasoft gluon field A^μ. Therefore the ultrasoft gluon interaction is provided by ultrasoft gauge invariance. Powers of μ_U^ϵ (as well as of μ_S^ϵ) are assigned to every effective theory operator unambiguously by considering its v-scaling. We do not write them down in the Lagrangian explicitly. Apart from that the terms for the ultrasoft ghost and massless quark fields are not shown explicitly.

The term δm_t is a residual mass term, present if a threshold mass scheme is used. It reduces the intrinsic ambiguity [58, 59] of order $\Lambda_{\rm QCD}$ of the pole mass (m_t) definition to a size that is parametrically below $\Lambda_{\rm QCD}$. Threshold mass definitions that have been used in the literature are e. g. the kinetic mass [60], the potential subtracted mass [61] (see also [62]) and the $1S$ mass [40, 63]. We will use the $1S$ mass scheme in the numerical analysis in Chap. 4.

In Eq. (1.3) we added for convenience to the ultrasoft QCD Lagrangian the electroweak matching condition $\propto i\Gamma_t$, which at LL effectively shifts the kinetic energy into the complex plane, $E \to E + i\Gamma_t$.

The soft piece of the Lagrangian reads

$$\begin{aligned}\mathcal{L}_s = \sum_q \big\{ |q^\mu A^\nu_q - q^\nu A^\mu_q|^2 + \bar\varphi_q \not{q} \varphi_q + \bar c_q q^2 c_q \big\} \\ - g_s^2 \sum_{\mathbf{p},\mathbf{p}',q,q',\sigma} \Big\{ \frac{1}{2} \psi^\dagger_{\mathbf{p}'} [A^\mu_{q'}, A^\nu_q] U^{(\sigma)}_{\mu\nu} \psi_{\mathbf{p}} + \frac{1}{2} \psi_{\mathbf{p}'} \{A^\mu_{q'}, A^\nu_q\} W^{(\sigma)}_{\mu\nu} \psi_{\mathbf{p}} \\ + \psi^\dagger_{\mathbf{p}'} [\bar c_{q'}, c_q] Y^{(\sigma)} \psi_{\mathbf{p}} + (\psi^\dagger_{\mathbf{p}'} T^B Z^{(\sigma)}_\mu \psi_{\mathbf{p}})(\bar\varphi_{q'} \gamma^\mu T^B \varphi_q) \Big\} + (\psi \to \chi, T \to \bar T) \,,\end{aligned}$$

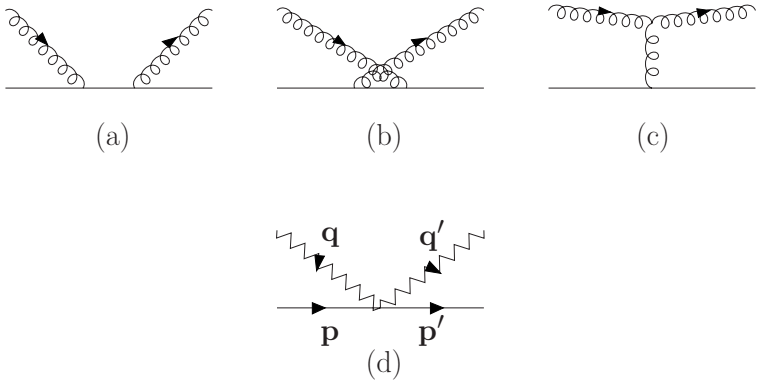

Figure 1.3: Compton scattering diagrams (a, b, c) in full QCD generate the soft interaction indicated in diagram (d). The zigzag lines denote soft gluons.

where A_q^μ, c_q and φ_q are gluon, ghost and massless quark fields of the soft 4-momentum q, respectively, and $g_u = g_u(\mu_S)$ is the soft QCD coupling. The matrices T^A denote the SU(3) generators, $\bar{T}^A$ is defined as $\bar{T}^A = -(T^A)^*$ and we use the symbol f^{ABC} for the SU(3) structure constants. The soft interaction terms generate diagrams of the form shown in Fig. 1.3 (d). The tensors $U_{\mu\nu}^{(\sigma)}$, $W_{\mu\nu}^{(\sigma)}$, $Z_{\mu\nu}^{(\sigma)}$ and $Y_{\mu\nu}^{(\sigma)}$, where the index σ denotes the relative order in the v expansion, are functions of $\mathbf{p}'$, $\mathbf{p}$, q', q and matrices in spin. They are fixed at the hard scale by integrating out the off-shell quarks and gluons in the full QCD diagrams (a, b, c) in Fig. 1.3 and the analogous ones with external ghosts and massless quarks. Their explicit form is given in Ref. [26].

Finally, the potential part of the Lagrangian reads

$$\begin{aligned}\mathcal{L}_p = &-\sum_{\mathbf{p},\mathbf{p}'} V_{\alpha\beta\lambda\tau}(\mathbf{p},\mathbf{p}')\psi^\dagger_{\mathbf{p}'\alpha}\psi_{\mathbf{p}\beta}\chi^\dagger_{-\mathbf{p}'\lambda}\chi_{-\mathbf{p}\tau} \\ &+\sum_{\mathbf{p},\mathbf{p}'} F_j^{ABC}(\mathbf{p},\mathbf{p}')(g_u\mathbf{A}_j^C)\left[\psi^\dagger_{\mathbf{p}'}T^A\psi_{\mathbf{p}}\chi^\dagger_{-\mathbf{p}'}\bar{T}^B\chi_{-\mathbf{p}}\right]+\dots \end{aligned} \tag{1.4}$$

with $(\mathbf{k} = \mathbf{p}' - \mathbf{p})$

$$\begin{aligned}V(\mathbf{p},\mathbf{p}') = (T^A\otimes\bar{T}^A)\Bigg[&\frac{\mathcal{V}_c^{(T)}}{\mathbf{k}^2}+\frac{\mathcal{V}_k^{(T)}\pi^2}{m_t|\mathbf{k}|}+\frac{\mathcal{V}_r^{(T)}(\mathbf{p}^2+\mathbf{p}'^2)}{2m_t^2\mathbf{k}^2}+\frac{\mathcal{V}_2^{(T)}}{m_t^2} \\ &+\frac{\mathcal{V}_s^{(T)}}{m_t^2}\mathbf{S}^2+\frac{\mathcal{V}_\Lambda^{(T)}}{m_t^2}\Lambda(\mathbf{p}',\mathbf{p})+\frac{\mathcal{V}_t^{(T)}}{m_t^2}T(\mathbf{k})+\dots\Bigg] \\ +(1\otimes 1)\Bigg[&\frac{\mathcal{V}_c^{(1)}}{\mathbf{k}^2}+\frac{\mathcal{V}_k^{(1)}\pi^2}{m_t|\mathbf{k}|}+\frac{\mathcal{V}_2^{(1)}}{m_t^2}+\frac{\mathcal{V}_s^{(1)}}{m_t^2}\mathbf{S}^2+\dots\Bigg],\end{aligned}$$

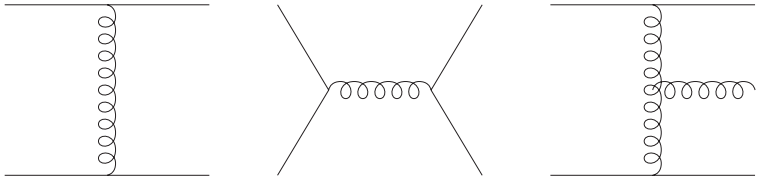

Figure 1.4: QCD diagrams that generate vNRQCD potentials.

$$\mathbf{S} = \frac{\boldsymbol{\sigma}_1 + \boldsymbol{\sigma}_2}{2}\,, \quad \Lambda(\mathbf{p}', \mathbf{p}) = -i\frac{\mathbf{S}\cdot(\mathbf{p}'\times\mathbf{p})}{\mathbf{k}^2}\,, \quad T(\mathbf{k}) = \boldsymbol{\sigma}_1\cdot\boldsymbol{\sigma}_2 - \frac{3\,\mathbf{k}\cdot\boldsymbol{\sigma}_1\,\mathbf{k}\cdot\boldsymbol{\sigma}_2}{\mathbf{k}^2}$$

and

$$F_j^{ABC}(\mathbf{p}, \mathbf{p}') = \frac{2i\mathcal{V}_c^{(T)}\mathbf{k}_j}{\mathbf{k}^4} f^{ABC}\,.$$

The operators $\boldsymbol{\sigma}_1/2$ and $\boldsymbol{\sigma}_2/2$ are the spin operators on top and antitop. The terms in $V(\mathbf{p}, \mathbf{p}')$ are the leading order Coulomb potential $\mathcal{V}_c$, the v^2-suppressed potentials contributing at $\mathcal{O}(\alpha_s)$ and the v-suppressed potential $\mathcal{V}_k$. The latter contributes at $\mathcal{O}(\alpha_s^2)$ since its tree level matching condition is zero, and hence it is also v^2-suppressed according to the v-counting $v \sim \alpha_s$. Matching to full QCD one-loop diagrams gives [64]

$$\mathcal{V}_k^{(T)} = \alpha_s^2(m_t)\left(\frac{7}{8}C_A - \frac{1}{8}C_d\right)\,, \qquad \mathcal{V}_k^{(1)} = \alpha_s^2(m_t)\frac{1}{2}\,C_1\,, \tag{1.5}$$

where C_F and C_A are the Casimir operators of the fundamental and the adjoint SU(3) representation, respectively. These and the constants C_1 and C_d are given in App. F. Apart from their dependence on the momenta, the potentials $\mathcal{V}_s$, $\mathcal{V}_\Lambda$ and $\mathcal{V}_t$ have a dependence on the spin of top and antitop.

The various coefficients are fixed at the hard scale m_t at order α_s by matching to full QCD tree level diagrams shown in Fig. 1.4. This leads to [26]

$$\begin{aligned}
&\mathcal{V}_c^{(T)} = 4\pi\alpha_s(m_t)\,, \quad \mathcal{V}_r^{(T)} = 4\pi\alpha_s(m_t)\,, \quad \mathcal{V}_s^{(T)} = -\frac{4\pi\alpha_s(m_t)}{3} + \frac{1}{N_c}\,\pi\alpha_s(m_t)\,,\\
&\mathcal{V}_\Lambda^{(T)} = -6\pi\alpha_s(m_t)\,, \quad \mathcal{V}_t^{(T)} = -\frac{\pi\alpha_s(m_t)}{3}\,, \quad \mathcal{V}_s^{(1)} = \frac{(N_c^2-1)}{2N_c^2}\,\pi\,\alpha_s(m_t)\,,\\
&\mathcal{V}_c^{(1)} = 0\,, \quad \mathcal{V}_2^{(T)} = 0\,, \quad \mathcal{V}_2^{(1)} = 0\,.
\end{aligned} \tag{1.6}$$

The basis in terms of $(1\otimes 1)$ and $(T^A\otimes\bar{T}^A)$ can be converted to the color singlet and octet basis by the linear transformation

$$\begin{bmatrix} V_{\text{singlet}} \\ V_{\text{octet}} \end{bmatrix} = \begin{bmatrix} 1 & -C_F \\ 1 & \frac{1}{2}C_A - C_F \end{bmatrix} \begin{bmatrix} V_{1\otimes 1} \\ V_{T\otimes T} \end{bmatrix}\,. \tag{1.7}$$

Since in our case the $t\bar{t}$ pair is produced from the intermediate photon or Z boson, we will concentrate only on the color singlet channel in this work.

At this point we give the expression for the LL evolution of $\mathcal{V}_r^{(s)}$ from Ref. [22] since it will contribute to the NLL running of forward scattering operators as we will see in Sec. 3.3,

$$\mathcal{V}_r^{(s)}(\nu) = -4\pi C_F \alpha_s(m_t) z \left[1 + \frac{8C_A}{3\beta_0}\ln(2-z)\right], \qquad z \equiv \frac{\alpha_s(m_t\nu)}{\alpha_s(m_t)}, \tag{1.8}$$

where β_0 is the $\mathcal{O}(\alpha_s^2)$ coefficient in the QCD β-function given in App. F and $n_f = 5$ is the number of light fermions.

The velocity power counting of the fields is derived from demanding that the action for the kinetic terms is of order v^0. One obtains

$$\begin{aligned} A_q^\mu &\sim v\,, \\ \psi_{\mathbf{p}} &\sim \chi_{\mathbf{p}} \sim v^{3/2}\,, \\ D^\mu &\sim A^\mu \sim v^2 \end{aligned} \tag{1.9}$$

for soft gluon fields, quark and antiquark fields, the (ultrasoft) covariant derivative and the ultrasoft gluon field, respectively.

1.4 Currents and Forward Scattering Operators

The components $\mathcal{L}_u$, $\mathcal{L}_s$ and $\mathcal{L}_p$ describe the non-relativistic $t\bar{t}$ dynamics due to the strong interaction once the heavy quark pair is produced. For the $t\bar{t}$ production itself one needs additional operators in the Lagrangian. For the treatment up to NNLL order in the cross section these are the dominant ${}^3S_1$ current $\mathcal{O}^j_{\mathbf{p},1}$, the subleading ($\mathbf{p}^2/m_t^2$-suppressed) ${}^3S_1$ current $\mathcal{O}^j_{\mathbf{p},2}$ and the leading ${}^3P_1$ current $\mathcal{O}^j_{\mathbf{p},3}$ [22], which is $\mathbf{p}/m_t$-suppressed compared to the dominant S-wave current. They have the form

$$\begin{aligned} \mathcal{O}^j_{\mathbf{p},1} &= \psi^\dagger_{\mathbf{p}}\,\sigma^j(i\sigma^2)\chi^*_{-\mathbf{p}}\,, \qquad \mathcal{O}^j_{\mathbf{p},2} = \frac{1}{m_t^2}\,\psi^\dagger_{\mathbf{p}}\,\mathbf{p}^2\,\sigma^j(i\sigma^2)\chi^*_{-\mathbf{p}}\,, \\ \mathcal{O}^j_{\mathbf{p},3} &= \frac{-i}{2m_t}\,\psi^\dagger_{\mathbf{p}}\,[\sigma^j, \boldsymbol{\sigma}\cdot\mathbf{p}]\,(i\sigma^2)\chi^*_{-\mathbf{p}}\,, \end{aligned} \tag{1.10}$$

$\mathbf{p}$ being the soft momentum label. In this basis of operators there is the additional D-wave current

$$\mathcal{O}^j_{\mathbf{p},4} = \frac{1}{m_t^2}\,\psi^\dagger_{\mathbf{p}}\,\left(p^j\,(\boldsymbol{\sigma}\cdot\mathbf{p}) - \sigma^j\mathbf{p}^2/3\right)\,(i\sigma^2)\chi^*_{-\mathbf{p}}\,,$$